THE ASTROPHYSICAL JOURNAL, 502:278–283, 1998 July 20

COSMIC-RAY PROTON AND HELIUM SPECTRA: RESULTS FROM THE JACEE EXPERIMENT

K. ASAKIMORI,[1] T. H. BURNETT,[2] M. L. CHERRY,[3] K. CHEVLI,[4] M. J. CHRIST,[5] S. DAKE,[6] J. H. DERRICKSON,[5] W. F. FOUNTAIN,[5] M. FUKI,[7] J. C. GREGORY,[4] T. HAYASHI,[8] R. HOLYNSKI[9], J. IWAI,[2] A. IYONO,[10] J. JOHNSON,[4] M. KOBAYASHI,[11] J. LORD,[2] O. MIYAMURA,[12] K. H. MOON,[5,13] B. S. NILSEN,[3,14] H. ODA,[6] T. OGATA,[15] E. D. OLSON,[2,16] T. A. PARNELL,[5] F. E. ROBERTS,[5] K. SENGUPTA,[3,17] T. SHIINA,[4] S. C. STRAUSZ,[2] T. SUGITATE,[12] Y. TAKAHASHI,[4] T. TOMINAGA,[12] J. W. WATTS,[5] J. P. WEFEL,[3] B. WILCZYNSKA,[9] H. WILCZYNSKI,[9] R. J. WILKES,[2] W. WOLTER,[9] H. YOKOMI,[18] AND E. ZAGER[2]

Received 1997 August 25; accepted 1998 February 19

ABSTRACT

Measurements of the cosmic-ray hydrogen and helium spectra at energies from 20 to 800 TeV are presented. The experiments were performed on a series of twelve balloon flights, including several long duration Australia to South America and Antarctic circumpolar flights. No clear evidence is seen for a spectral break. Both the hydrogen and the helium spectra are consistent with power laws over the entire energy range, with integral spectral indices 1.80 ± 0.04 and $1.68^{+0.04}_{-0.06}$ for the protons and helium, respectively. The results are fully consistent with expectations based on supernova shock acceleration coupled with a "leaky box" model of propagation through the Galaxy.

Subject headings: acceleration of particles — balloons — ISM: cosmic rays

1. INTRODUCTION

One of the striking features of high-energy cosmic rays is the power-law dependence of the observed flux on energy over approximately 10 orders of magnitude—from near 10^{10} eV where the Earth's geomagnetic field becomes transparent to the incident cosmic-ray beam to 3×10^{20} eV, the highest energy observed by the Fly's Eye experiment (Bird et al. 1993). In the middle of this wide range of energies, however, a "knee" is observed near 10^{15}–10^{16} eV where the spectrum steepens. It is not clear whether this steepening is due to

1. A change in the acceleration mechanism at the cosmic-ray source(s) possibly related to a maximum energy available from shock acceleration in galactic supernova remnants.
2. A change in the propagation mechanism, e.g., escape from the galaxy's magnetic fields.
3. A change in the elemental composition of the cosmic rays.
4. A change in the interaction characteristics owing to new particle physics at energies $s^{1/2}$ above 1 TeV nucleon^{-1}.
5. An observational bias related to a change in the experimental techniques from direct particle-by-particle balloon and spacecraft measurements below $\sim 10^{14}$ eV to indirect ground-based air shower measurements above 10^{15} eV.
6. Uncertainties in the energy determination and calibration of the air shower measurements.

In order to address these questions, provide overlap between the direct "low-energy" observations and the indirect "high-energy" measurements, and to anchor firmly the high-energy air shower measurements, it is necessary to push the balloon-borne direct measurements up in energy as far as possible. Long duration balloon (LDB) flights of large-area nuclear emulsion chambers provide the capability to perform this measurement almost to the knee region.

The high-energy cosmic-ray spectrum is relevant to understanding the acceleration mechanism(s) and conditions at the source(s), the propagation of the energetic cosmic rays through the galaxy, the cosmological issues of galactic versus extragalactic origin, and the particle physics of interactions in the Earth's atmosphere (and in the case of underground and underwater detectors, the Earth's surface and oceans). The steepening of the all-particle spectrum above the knee and the intensity enhancement observed below the knee (both derived indirectly from air shower data) have been the subject of numerous speculations on the acceleration and propagation mechanisms of galactic cosmic rays.

If these mechanisms depend on particle rigidity, a change in the proton energy spectrum is expected at an energy lower than that of any $Z > 1$ component and lower than any bend in the all-particle spectrum. The first measurements in the TeV region, made by the *PROTON* satellites (Grigorov et al. 1971), indicated that the proton integral spectral index changed from 1.7 to 2.1 at around 2 TeV and then remained constant up to at least 20 TeV. The later Japanese-American Cooperative Emulsion Experiment (JACEE) data (Burnett et al. 1983, 1990) showed no steepening up to approximately 100 TeV based on data from a series of six balloon flights. In 1991, however, JACEE reported preliminary results of the long duration

[1] Kobe Women's Junior College, Kobe, Japan.
[2] Department of Physics, University of Washington, Seattle, WA 98195.
[3] Department of Physics and Astronomy, Louisiana State University, Baton Rouge, LA 70803.
[4] College of Science, University of Alabama, Huntsville, AL 35899.
[5] NASA Marshall Space Flight Center, Huntsville, AL 35812.
[6] Kobe University, Kobe, Japan.
[7] Kochi University, Kochi, Japan.
[8] Waseda University, Tokyo, Japan.
[9] Institute for Nuclear Physics, Krakow, Poland.
[10] Okayama University of Science, Okayama, Japan.
[11] National Laboratory for High Energy Physics (KEK), Tsukuba, Japan.
[12] Hiroshima University, Hiroshima, Japan.
[13] Deceased.
[14] Present address: Ohio State University, Columbus, OH 43210.
[15] Institute for Cosmic Ray Research, Tokyo, Japan.
[16] Present address: WRQ, Inc., Seattle, WA 98109.
[17] Present address: Horizon Computer Corporation, 5 Lincoln Highway, Edison, NJ 08820.
[18] Tezukayama University, Nara, Japan.

Australia-to-South America JACEE 7 and 8 flights and showed that the proton flux above 80 TeV was almost three standard deviations below the intensity expected from a single power law (Asakimori et al. 1991). With the fully analyzed data from JACEE 7 and 8 (cumulative exposure 305 m^2-hrs), a "rollover" in the proton spectrum above ~ 40 TeV was indicated, but no complementary steepening was observed in the helium spectrum (Asakimori et al. 1993). The Sokol group (Ivanenko et al. 1990; Grigorov, 1990; Grigorov et al. 1990) reported a proton spectral index that steepened by approximately 1 σ between 2.5 and 10 TeV and a helium index that flattened by 1 σ in the same energy range. Other groups (Kawamura et al. 1989; Ivanenko et al. 1993; Zatsepin et al. 1993a, 1993b) have reported no steepening in the spectra, but have agreed that the H/He ratio decreases with increasing energy.

If a bend in the proton spectrum is interpreted as a result of a maximum rigidity for the acceleration process, then the helium should show a similar bend at a kinetic energy Z/A times the proton break energy; i.e., a bend in the proton spectrum near 40 TeV should appear in the helium spectrum near 20 TeV nucleon^{-1}. A steepening of the proton spectrum at some energy E_p without a corresponding steepening for helium could imply that the theoretical prediction for a maximum total energy nucleon$^{-1} \sim ZE_p/A$ from a supernova shock is oversimplified, or it could suggest that the protons and helium come from different sources. It was clearly recognized by Asakimori et al. (1993) that the JACEE 1–8 results were statistically limited, and that additional LDB exposures would be needed to address properly the question of the high-energy proton and helium spectra. We present here the results of the analysis through JACEE flight 12, with a factor of 2 more data than were available through JACEE 8 and with an improved treatment of systematic effects. The present results update and replace our earlier JACEE proton and helium results.

2. EXPERIMENTAL PROCEDURE

Nuclear emulsion has the advantage that relatively light, large-area, passive payloads can be flown on high-altitude balloons. In order to accumulate the required high-energy statistics, JACEE has now flown emulsion chambers on 15 balloon flights (eight 1–2 day turnaround flights, two 5–6 day Australia-South America flights, and five 9–15 day Antarctic circumpolar flights; Wilkes et al. 1995). All but one of these have been successfully recovered. The total accumulated exposure is 1436 m^2-hrs (Table 1). The average flight altitude ranges from 3.5 to 5.5 g cm^{-2}. A single flight typically carries 2–6 emulsion blocks, each generally 40×50 cm^2. Fifty-eight emulsion blocks have been flown; 52 have been recovered. We report here the analysis of the data from JACEE flights 1–12, covering the results from the first 40 emulsion blocks (cumulative exposure 644 m^2-hrs). The total number of high-energy events available for analysis from all flights is $\sim 2 \times 10^4$. Of these, ~ 180 have energy exceeding 100 TeV per particle. The present analysis is based on 656 protons above 6 TeV and 414 helium nuclei above a total energy of 8 TeV per particle.

The basic detector used in the JACEE experiments (Burnett et al. 1986; Fig. 1) is a fine-grained emulsion chamber containing approximately a hundred track-sensitive nuclear emulsion plates and a three-dimensional emulsion/X-ray film/lead plate calorimeter. (JACEE 3 was a hybrid experiment that combined the standard emulsions with a set of electronic Cerenkov detectors, proportional and ionization chambers, and a plastic shower counter in order to test the validity of the emulsion chamber approach).

The lower part of the chamber is the calorimeter section, consisting of ~ 20 layers of emulsions and X-ray films interleaved with up to 8.5 radiation lengths of 1–2.5 mm thick lead plates. The calorimeter records single-charged particle tracks with a spatial resolution in the emulsion of better than 1 μm and individual photon cascades with a resolution of a few microns. High-energy showers produce visible dark spots in the X-ray film, which are used to locate and trace the energetic cascades. On average, more than 400 events are detected per block with optical density in the electromagnetic cascade ($D_{\max}$ for a slit size of 200 μm $\times$ 200 μm) greater than 0.2, corresponding to a total energy in the electromagnetic shower $\Sigma E_\gamma \geq 1.5$ TeV for protons. In the original JACEE analyses (Burnett et al. 1986, 1990; Asakimori et al. 1991, 1993), electron counts in the emulsion layers along the cascade were compared to a simulated shower development curve to determine the total electro-

TABLE 1

JACEE BALLOON FLIGHTS

JACEE FLIGHT	LAUNCH DATE	LAUNCH SITE	ALTITUDE (g cm^{-2})	DURATION (hr)	UNITS (cm $\times$ cm)	CUMULATIVE EXPOSURE (m^2-hrs)
0	1979 May	Sanriku, Japan	8.0	29.0	1(40 $\times$ 50)	6
1	1979 Sept	Palestine, TX	3.7	25.2	4(40 $\times$ 50)	26
2	1980 Oct	Palestine, TX	4.0	29.6	4(40 $\times$ 50)	50
3	1982 Jun	Greenville, C	5.0	39.0	1(50 $\times$ 50)	59
4	1983 Sept	Palestine, TX	5.0	59.5	4(40 $\times$ 50)	107
5	1984 Oct	Palestine, TX	5.0	15.0	4(40 $\times$ 50)	119
6	1986 May	Palestine, TX	4.0	30.0	4(40 $\times$ 50)	143
7	1987 Jan	Alice Springs, Australia	5.5	150.0	3(40 $\times$ 50)	233
8	1988 Feb	Alice Springs	5.0	120.0	3(40 $\times$ 50)	305
9	1990 Oct	FT. Sumner, NM	4.0	44.0	4(40 $\times$ 50)	340
10	1990 Dec	McMurdo, Antarctica	3.5	204.0	2(30 $\times$ 40)	389
11	1993 Dec	McMurdo	4.5	217.0	6(40 $\times$ 50)	[a]
12	1994 Jan	McMurdo	5.0	212.0	6(40 $\times$ 50)	644
13	1994 Dec	McMurdo	5.0	310.0	6(40 $\times$ 50)	1016
14	1995 Dec	McMurdo	5.0	350.0	6(40 $\times$ 50)	1436

[a] JACEE 11 was lost in the ocean because of a malfunction at cutdown after a nine-day flight.

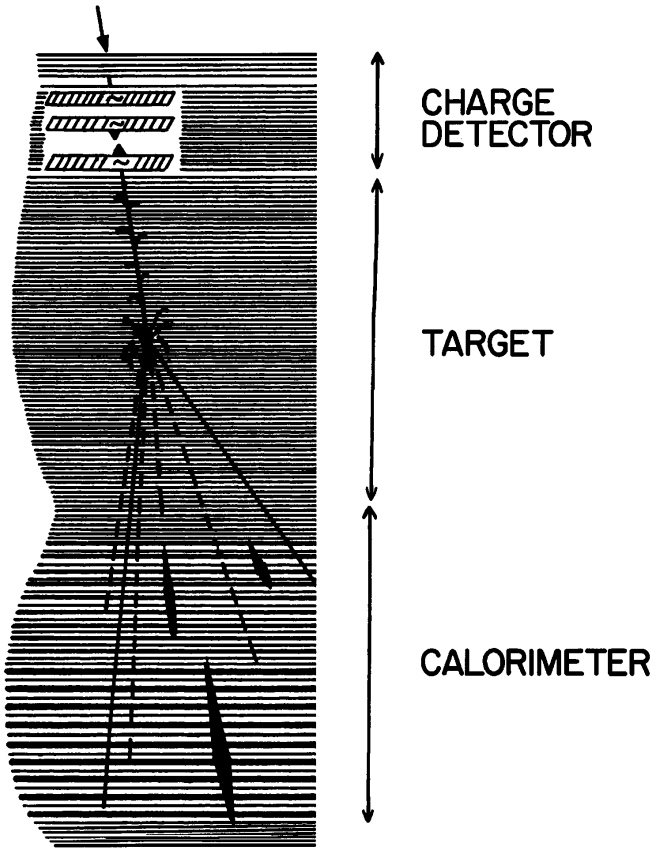

FIG. 1.—Schematic diagram of the JACEE experimental configuration

magnetic energy ΣE_γ deposited in the calorimeter. The electron counting in the emulsion is a slow, manual, manpower-intensive operation. In order to speed up the analysis for the large new data sample obtained from our long duration Antarctic flights, we have derived ΣE_γ directly from the darkness D measured in the X-ray films. X-ray film optical density is defined in terms of the fraction of incident light intensity transmitted through a sample

$$D = -\log I/I_0 \, . \tag{1}$$

Measured film density D is then related to the density of electron tracks n in an adjacent emulsion plate by the empirical relation (Ohta et al. 1979)

$$D = D_0\left(1 - \frac{1}{1 + \alpha n}\right), \tag{2}$$

where the constant D_0 is determined from measurements with a calibration wedge and α is determined by a calibration of D with direct counting of the shower electron density. The net density or "darkness" due to a shower electron density n_s, superposed on a background n_b, is

$$D_{\rm net} = D_{\rm total} - D_{\rm bkg} = D_0\left[\frac{1}{1 + \alpha n_b} - \frac{1}{1 + \alpha(n_s + n_b)}\right], \tag{3}$$

where the background density n_b is determined from equation (2), with $n = n_b$ and $D = D_{\rm bkg}$ measured away from the shower spot. The shower electron density is determined at various points along the track of the shower either directly by counting in the emulsion or indirectly from the X-ray film darkness. Corrections are made for the non-vertical angles, the shadowing of the bottom layer of the film by the top layer, and the finite film thickness; n_s is then fitted to the electromagnetic shower development curves in order to determine ΣE_γ (Burnett et al. 1986; Olson 1995).

A correction must be made for both background and saturation in the X-ray film densitometry. This is especially important for the Antarctic LDB flights. where fogging due to the low geomagnetic cutoff rigidity, the long flight duration, and, in a few cases, somewhat old X-ray films tended to increase the background levels and decrease dynamic range. We use neutral density filters to increase the dynamic range. In the absence of filtering, $D_0 = 4.2$ because of photomultiplier saturation; with proper filters, $D_0 \geq 6.5$ because of film saturation. For JACEE 12, the observed background level was $D_{\rm bkg} \sim 1.6$ (higher by 0.5–1 unit than in previous flights). Therefore, in order to reduce the effect of saturation, all high-D JACEE 12 showers were measured with a $D = 1.4$ filter.

It should be noted that the definition of n_s in terms of the net darkness in equation 3 is somewhat different from the standard convention, where $D_{\rm net}$ is set equal to D in equation 2 (Ohta et al. 1979; Okamoto et al. 1981; Kasahara et al. 1985; Kawamura et al. 1989). The two definitions give similar numerical results for $\alpha n_b \ll 1$. For high-energy measurements that employ data from long duration balloon or mountaintop exposures, however, the use of the proper characteristic curve (eq. [3]) for $D_{\rm net}(n_s)$, is important. As an example, for a long duration JACEE 12 data sample with $D_{\rm bkg} = 1.6$ and $D_{\rm net} = 1.0$, the darkness calculation without the background correction (e.g., eq. [2]) underestimates ΣE_γ by 4%. At $D_{\rm net} = 1.2$, however, there is a 30% underestimate for vertically incident particles and 21% underestimate for particles with zenith angle $\theta = 79°$ ($\tan\theta = 5.0$). The characteristic curve without background correction has been used by the JACEE group for the analysis of its shorter flights until 1993. In the present analysis, the data have been reanalyzed using the correct expression (eq. [3]) for all values of darkness.

In practice, the value determined from the densitometry is the maximum darkness $D_{\rm max}$, i.e., the film darkness at shower maximum. However, the parameter α used in converting $D_{\rm max}$ to electron counts (eqs. [2] and [3]) depends on the primary particle's angle of incidence. At darkness values near threshold, the cutoff is therefore dependent on the angle of incidence, and an energy-dependent efficiency correction must be applied, resulting in a background density-dependent effective threshold $\Sigma E_{\gamma,\rm thresh} \sim 700$ GeV ($D_{\rm max} \sim 0.1$). The correction for incident direction becomes independent of energy above $\Sigma E_\gamma \sim 4$ TeV. Since the tracing of each event through the emulsion layers is time-consuming, only high-energy events are selected for analysis. The selection criteria require a minimum $D_{\rm max}$ ranging from 0.2 for JACEE 1–6 to 0.5 for JACEE 12. Zenith angle θ, azimuth angle ϕ, and optical density $D_{\rm max}$ are recorded for all selected events. A zenith angle cut is applied for each flight; typically $\tan\theta \leq 5.0$ ($\theta \leq 79°$) for high-energy events ($D_{\rm max} \geq 0.5$) and $\tan\theta \leq 3.0$ ($\theta \leq 72°$) for events with $D_{\rm max} < 0.5$. With these selection criteria, the effective solid angle acceptance of the chamber remains very high ($\sim$3–3.5 sr) compared to that for a typical electronic calorimeter experiment ($\sim$0.1 sr).

A comparison of ΣE_γ values determined from direct electron counting to those derived from the X-ray film densitometry (Olson 1995; Cherry et al. 1995) gives a dispersion

in the individual event ΣE_γ values of approximately 30% between the two methods. Shower-to-shower fluctuations (including the event-to-event variations in interaction height and the variations owing to the width of the inelasticity distribution in nucleon-nucleus interactions) have been studied using Monte Carlo simulations (Burnett et al. 1986). The standard deviations of the relative widths derived from the simulations are 18% and 23% for protons and helium, respectively, resulting in a net uncertainty $(\delta\Sigma E_\gamma)/\Sigma E_\gamma \sim 35\%$–$38\%$.

Since the cosmic-ray spectrum is approximately a power law decreasing rapidly with increasing energy, this uncertainty in the measured energy ΣE_γ means that low-energy particles will be preferentially misidentified as higher energy particles. If the "real" ΣE_γ spectrum is denoted $dN/d\epsilon$, then the observed spectrum will be the convolution of $dN/d\epsilon$ with a resolution function (assumed to be Gaussian)

$$\frac{dN}{d\Sigma E_\gamma} = \int_0^\infty \frac{dN}{d\epsilon} \frac{e^{-(\epsilon - \Sigma E_\gamma)^2/2\sigma^2}}{\sqrt{2\pi}\sigma} d\epsilon , \tag{4}$$

where the proton (helium) resolution is $\sigma = 0.35(0.38)\epsilon$. In the case of a power-law input spectrum with integral spectral index γ between 2 and 3, the integration in equation (4) is carried out numerically and results in a correction to the normalization of approximately 4%–11%.

The measured energy ΣE_γ is related to the primary energy E by the partial inelasticity k. Since the inelasticity distribution $f(k)$ has a width $\sim 50\%$, it is not possible to determine accurately the primary energy E of an individual event. There is, however, a well-defined relation between the ΣE_γ spectrum and the primary spectrum (Burnett et al. 1986; Kawamura et al. 1989). As long as the primary spectrum does not change slope and there is no change in the interaction characteristics over the energy range being considered, the primary spectrum and the ΣE_γ spectrum will be parallel. The primary spectrum can be determined from the ΣE_γ spectrum by a simple scale shift: If the primary spectrum is of the form

$$dN/dE = I_0 E^{-(\gamma+1)} , \tag{5}$$

then the measured spectrum will be

$$\begin{aligned} \frac{dN}{d\Sigma E_\gamma} &= \int_0^\infty \int_0^1 f(k) dk \delta(\Sigma E_\gamma - kE) I_0 E^{-(\gamma+1)} dE \\ &= I_0 \Sigma E_\gamma^{-(\gamma+1)} \int_0^1 k^\gamma f(k) dk . \end{aligned} \tag{6}$$

The measured spectrum therefore has the same slope as the primary spectrum, but with a normalization that differs by a factor C^γ, where

$$C(k, \gamma) = \left[\int_0^1 k^\gamma f(k) dk \right]^{1/\gamma} . \tag{7}$$

$C(k, \gamma)$ represents the shift in the energy scale required to go from the primary spectrum to the measured $\Sigma E_\gamma = C(k, \gamma) E$ spectrum. In the case where the spectral index changes, the dN/dE and $dN/d\Sigma E_\gamma$ spectra are parallel above and below the break enegy, and the energy of the break shifts by $\sim 10\%$–20%. For the measured JACEE spectra presented in § 3, the $C(k, \gamma)$ values for events interacting in the JACEE target section are 0.265 and 0.168 for protons and helium, respectively. For events interacting in the calorimeter, the $C(k, \gamma)$ values are $\sim 10\%$ higher.

The primary particle charge is measured by grain or gap counting by using a combination of low- (Fuji 6B) and high-sensitivity (Fuji 7B) emulsions in the upper portion of the chamber (Burnett et al. 1986, 1990). The measurement accuracy is $\delta Z = 0.2e$ for both protons and helium. The discrimination of protons from helium is made with close to 100% efficiency. We note that some other emulsion chamber experiments do not have this capability. In JACEE, the use of background nuclei as fiducials makes possible a precision triangulation of the event axis. The resulting error in locating the primary track in the emulsion plates is ~ 10 μm, so that there are practically no spurious background tracks with the same (θ, ϕ) values within this small area, and the identification of protons and helium is essentially unique at all angles.

3. RESULTS AND DISCUSSION

Figure 2 shows the measured JACEE 1–12 integral spectra $N(>E)$ for hydrogen and helium, including an atmospheric correction and corrections for the interaction height, target volume, and geometry for each particular event. Each point on the plot corresponds to one more event than the point to the right. The wavy shape of the low-statistics high-energy points (e.g., the dip in the proton spectrum between 60 and 100 TeV and in the helium spectrum near 20–30 TeV) is characteristic of the point-to-point correlations in an integral plot. The straight lines shown in Figure 2 are the maximum likelihood fits with power-law indices.

$$\gamma_{\rm H} = 1.80 \pm 0.04 \quad \gamma_{\rm He} = 1.68^{+0.04}_{-0.06} . \tag{8}$$

The JACEE 1–12 data are consistent with a single power law over the entire energy range. With the increased statistics, although we cannot rule out the two-component spectrum of Asakimori et al. (1993), we nevertheless see no evidence for a break in the spectrum. The hydrogen spectrum appears to be steeper than that of the helium, with a difference between the spectral indices of 0.12 ± 0.06.

The differential spectra dN/dE shown in Figure 3 demonstrate that the normalization agrees with the lower energy data. The solid lines shown in Figure 3 are the fits to the JACEE spectra:

$$\begin{aligned} \left.\frac{dN}{dE}\right|_{\rm H} &= (1.11^{+0.08}_{-0.06}) \times 10^{-1} E^{-2.80 \pm 0.04} \\ &\quad {\rm m^{-2}\ sr^{-1}\ s^{-1}\ TeV^{-1}} , \\ \left.\frac{dN}{dE}\right|_{\rm He} &= (7.86 \pm 0.24) \times 10^{-3} E^{-2.68^{+0.04}_{-0.06}} \\ &\quad {\rm m^{-2}\ sr^{-1}\ s^{-1}\ TeV^{-1}} . \end{aligned} \tag{9}$$

If we assume a standard "leaky box" model for the cosmic-ray propagation (Ormes & Freier 1978; Cesarsky 1980), then the measured secondary-to-primary cosmic-ray ratios lead to an energy-dependent cosmic-ray pathlength through the Galaxy (Garcia-Munoz et al. 1984, 1987; Guzik & Wefel 1984), for example

$$\lambda = \lambda_0 \left(\frac{R}{R_0} \right)^{-\delta} + \lambda_1 , \tag{10}$$

where $R = pc/Ze$ is the particle rigidity, $\lambda_0 = 6$ g cm^{-2}, $R_0 = 10$ GV, and $\delta = 0.6$. The constant term λ_1 is required

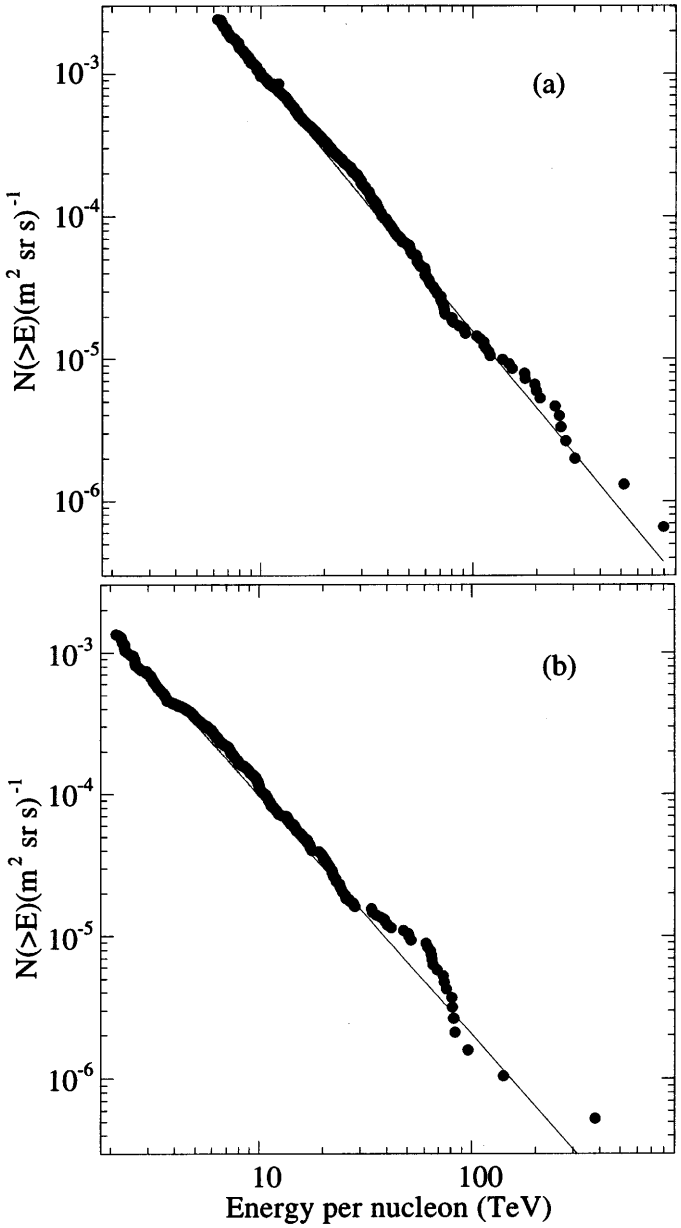

FIG. 2.—Measured JACEE 1–12 integral spectrum $N(>E)$ for hydrogen (*a*) and helium (*b*).

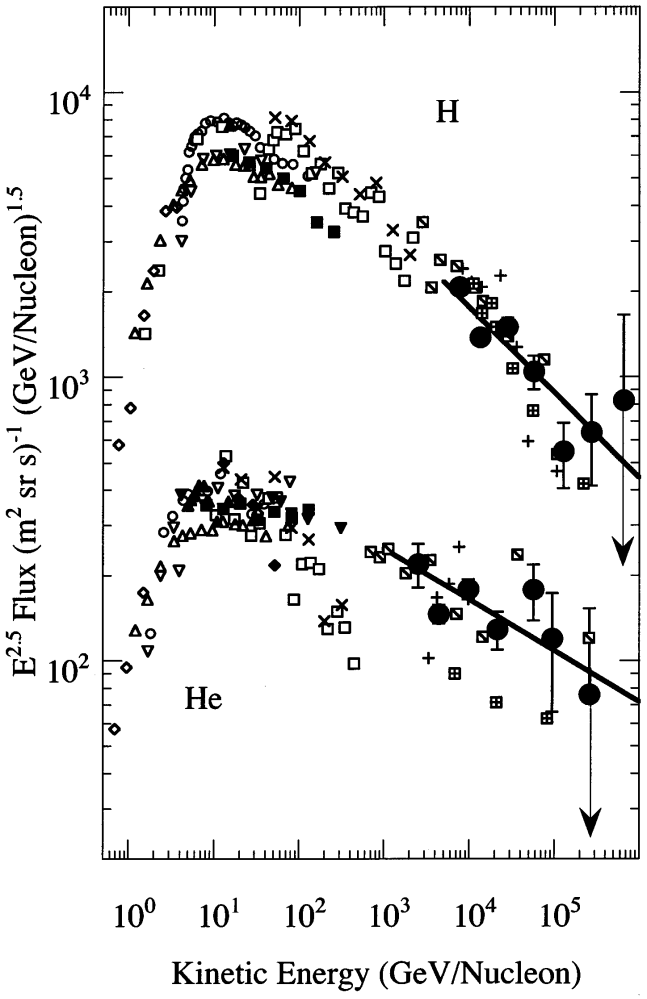

FIG. 3.—Differential spectra dN/dE showing present results (*filled circles*) together with earlier results from Freier & Waddington (1968, *open diamonds*), Anand et al. (1968, *upward pointing filled triangle*), Ryan et al. (1972, *crosses*), Verma et al. (1972, *filled diamonds*), Ramaty et al. (1973, *open squares*), Smith et al. (1973, *downward pointing open triangle*), Badhwar et al. (1977, *open circles*), Seo et al. (1991, *upward pointing open triangles*), Dwyer et al. (1993, *downward pointing filled triangle*), Ichimura et al. (1993, *plus signs*), Ivanenko et al. (1993, *open squares with diagonal lines*), Zatsepin et al. (1993, *open squares with cross*), and Swordy et al. (1995, *filled squares*).

by the absence of anisotropy at high energies (Swordy 1995). At energies in the TeV range, where the pathlength λ is small compared to the interaction mean free path, the leaky box model predicts hydrogen and helium spectra of the form $dN/dE \sim \lambda E^{-\alpha}$, where $E^{-\alpha}$ is the source spectrum. As long as λ_1 is small compared to $\lambda_0(R/R_0)^{-\delta}$, the spectra should be of the form $dN/dE \sim E^{-\alpha-0.6}$. The measurements therefore suggest source spectra of the form

$$\left.\frac{dN}{dE}\right|_{\text{source,H}} \sim E^{-2.2} \quad \left.\frac{dN}{dE}\right|_{\text{source,He}} \sim E^{-2.1} . \qquad (11)$$

A helium spectrum slightly flatter than that of the hydrogen is consistent with both the nonlinear shock acceleration calculations of Ellison (1993) and the multiple source models of Biermann (1993) and others, which suggest supernova remnant shock acceleration from a supernova exploding into the interstellar medium to explain the hydrogen spectrum, and a supernova exploding into the stellar wind of the pre-supernova star (e.g., a Wolf-Rayet star) to explain the high-energy helium.

At the energy where $\lambda_1 \sim \lambda_0(R/R_0)^{-\delta}$, the presence of the constant term λ_1 in equation (11) implies that both the hydrogen and the helium spectra should flatten to $dN/dE \sim E^{-\alpha}$. As long as the shock acceleration region is sufficiently large that the accelerator has not yet reached its maximum energy, the spectra will flatten toward the source spectra. The absence of any observed flattening by 200 TeV implies that $\lambda_1 < 0.016$ g cm^{-2}.

The maximum proton energy expected from acceleration at a parallel shock, assuming the standard value of 3 μG for the interstellar magnetic field, is $E_p \sim 100$ TeV (Lagage & Cesarsky 1983a, 1983b). This value can be extended upward by employing quasi-perpendicular shocks (Jokipii 1987) or higher magnetic fields as might be encountered by a supernova remnant expanding into the wind of a massive progenitor star (Völk & Biermann 1988). Likewise, reacceleration by multiple supernova remnants (Axford

1991) or a Galactic termination shock (Jokipii & Morfill 1991) might significantly increase E_p. The absence of a spectral break in the present results near 100 TeV can therefore be readily accommodated by extensions to the original Lagage & Cesarsky (1983a, 1983b) model.

4. CONCLUSIONS

The JACEE results represent the highest energy direct particle-by-particle measurements available on the spectrum of cosmic-ray hydrogen and helium up to 800 TeV. With 644 m^2-hrs of accumulated exposure (including the results from two greater than 200 hr Antarctic flights), we have measured 656 proton events above 6 TeV and 414 heliums above 2 TeV nucleon^{-1}. The resulting spectra are consistent with power laws with no spectral breaks. The hydrogen spectral index is steeper than that of the helium by 0.12, corresponding to 2 σ. With the improved statistics from the Antarctic flights, the results appear to be consistent with the predictions based on models of supernova shock acceleration and leaky box propagation.

This work has been supported in the US by NASA (Space Physics, EPSCoR), the National Science Foundation (Particle Physics, Polar Programs, EPSCoR), Department of Energy (High Energy Physics), the State of Alabama EPSCoR program, and the Louisiana Board of Regents; in Japan by the Institute for Cosmic Ray Research, University of Tokyo, Japan Society for Promotion of Science, Yamada Science Foundation, and the Kashima Foundation; and in Poland by the Polish State Committee for Scientific Research and the Maria Sklodowska-Curie Fund (grants 2P03B18109) and PAA-NSF-96-256). We appreciate the extensive microscope work by A. Aranas, B.-L. Dong, and S. Toyoda.

REFERENCES

Anand, K. C., et al. 1968, Canad. J. Phys., 46, 5652
Asakimori, K., et al. 1991, Proc. 22d Int. Cosmic Ray Conf. (Dublin), 2, 97
———. 1993, Proc. 23d Int. Cosmic Ray Conf. (Calgary), 2, 21, and 2, 25
Axford, W. I. 1991, in Astrophysical Aspects of the Most Energetic Cosmic Rays, ed. M. Nagano & F. Takahara (World Scientific: Singapore), 406
Badhwar, G. D., et al. 1977, Proc. 15th Int. Cosmic Ray Conf. (Plovdiv), 11, 155
Biermann, P. L. 1993, Astron. Astrophys., 271, 649; P. L. Biermann & J. P. Cassinelli, 1993, Astron. Astrophys., 277, 691
Biermann, P. L., & Strom, R. G. 1993, A&A, 275, 659
Bird, D. J., et al. 1993, Phys. Rev. Lett., 71, 3401
Burnett, T. H., et al. 1983, Phys. Rev. Lett., 51, 1010
———. 1986, Nucl. Instrum. Methods Phys. Res., A251, 583
———. 1990, ApJ, 349, 25
Cesarsky, C. J. 1980, ARA&A, 18, 289
Cherry, M. L., et al. 1995, Proc. 24th Int. Cosmic Ray Conf. (Rome), 2, 728
Dwyer, J., et al. 1993, Proc. 23d Int. Cosmic Ray Conf. (Calgary), 1, 587
Ellison, D. C. 1993, Proc. 23d Int. Cosmic Ray Conf. (Calgary), 2, 219
Freier, P. S., & Waddington, C. J. 1968, J. Geophys. Res., 264, 4261
Garcia-Munoz, M., et al. 1984, ApJ, 280, L13
———. 1987, ApJS, 64, 269
Grigorov, N. L. 1990a, Sov. J. Nucl. Phys., 51, 99
Grigorov, N. L., et al. 1971, Proc. 12th Int. Cosmic Ray Conf. (Hobart), 5, 1746
———. 1990b, Proc. 21st Int. Cosmic Ray Conf. (Adelaide), 3, 73
Guzik, T. G., & Wefel, J. P. 1984, Adv. Space Res., 4(2), 215
Ichimura, M., et al. 1993, Phys. Rev. D, 48, 1949
Ivanenko, I. P., et al. 1990, Proc. 21st Int. Cosmic Ray Conf. (Adelaide), 3, 77
Ivanenko, I. P., et al. 1993, Proc. 23d Int. Cosmic Ray Conf. (Calgary), 2, 17
Jokipii, J. R. 1987, ApJ, 313, 842
Jokipii, J. R., & Morfill, G. 1991, in Astrophysical Aspects of the Most Energetic Cosmic Rays, ed. M. Nagano & F. Takahara (World Scientific: Singapore), 261
Kasahara, K., et al. 1985, Phys. Rev. D, 31, 2737
Kawamura, Y., et al. 1989, Phys. Rev. D, 40, 729
Lagage, P. O., & Cesarsky, C. J. 1983a, A&A, 118, 223
———. 1983b, A&A, 125, 249
Ohta, I., et al. 1979, Nucl. Instrum. Methods Phys. Res., 161, 35
Okamoto, T., et al. 1981, Proc. 17th Int. Cosmic Ray Conf. (Paris), 5, 214, 218, 222
Olson, E. D. 1995, Ph.D. thesis, Univ. Washington
Ormes, J. F., & Freier, P. S. 1978, ApJ, 222, 471
Ramaty, R., et al. 1973, Science, 180, 731
Ryan, M. J., et al. 1972, Phys. Rev. Lett., 28, 985
Seo, E. S., et al. 1991, ApJ, 378, 763
Smith, L. H., et al. 1973, ApJ, 180, 978
Swordy, S. P. 1995, Proc. 24th Int. Cosmic Ray Conf. (Rome), 2, 697
Swordy, S. P., et al. 1995, Proc. 24th Int. Cosmic Ray Conf. (Rome), 2, 652
Verma, R. P., et al. 1972, Nature, 240, 135
Völk, H. J., & Biermann, P. L. 1988, ApJ, 333, L265
Wilkes, R. J., et al. 1995, Proc. 24th Int. Cosmic Ray Conf. (Rome), 3, 615
Zatsepin, V. I., et al. 1993a, Proc. 23d Int. Cosmic Ray Conf. (Calgary), 2, 13
———. 1993b, Proc. 23d Int. Cosmic Ray Conf. (Calgary), 5, 439